NASA/TM-20210021120 AIAA–2021–2649

Isokinetic Probe Total Water Content Measurements in the NASA Icing Research Tunnel With Supercooled Large Drop Conditions

Thomas P. Ratvasky
Glenn Research Center, Cleveland, Ohio

J. Walter Strapp
Met Analytics, Inc., Aurora, Ontario, Canada

Lyle E. Lilie
Science Engineering Assoc., Tolland, Connecticut

November 2021

NASA STI Program . . . in Profile

Since its founding, NASA has been dedicated to the advancement of aeronautics and space science. The NASA Scientific and Technical Information (STI) Program plays a key part in helping NASA maintain this important role.

The NASA STI Program operates under the auspices of the Agency Chief Information Officer. It collects, organizes, provides for archiving, and disseminates NASA's STI. The NASA STI Program provides access to the NASA Technical Report Server—Registered (NTRS Reg) and NASA Technical Report Server—Public (NTRS) thus providing one of the largest collections of aeronautical and space science STI in the world. Results are published in both non-NASA channels and by NASA in the NASA STI Report Series, which includes the following report types:

- TECHNICAL PUBLICATION. Reports of completed research or a major significant phase of research that present the results of NASA programs and include extensive data or theoretical analysis. Includes compilations of significant scientific and technical data and information deemed to be of continuing reference value. NASA counter-part of peer-reviewed formal professional papers, but has less stringent limitations on manuscript length and extent of graphic presentations.

- TECHNICAL MEMORANDUM. Scientific and technical findings that are preliminary or of specialized interest, e.g., "quick-release" reports, working papers, and bibliographies that contain minimal annotation. Does not contain extensive analysis.

- CONTRACTOR REPORT. Scientific and technical findings by NASA-sponsored contractors and grantees.

- CONFERENCE PUBLICATION. Collected papers from scientific and technical conferences, symposia, seminars, or other meetings sponsored or co-sponsored by NASA.

- SPECIAL PUBLICATION. Scientific, technical, or historical information from NASA programs, projects, and missions, often concerned with subjects having substantial public interest.

- TECHNICAL TRANSLATION. English-language translations of foreign scientific and technical material pertinent to NASA's mission.

For more information about the NASA STI program, see the following:

- Access the NASA STI program home page at http://www.sti.nasa.gov

- E-mail your question to help@sti.nasa.gov

- Fax your question to the NASA STI Information Desk at 757-864-6500

- Telephone the NASA STI Information Desk at 757-864-9658

- Write to:
  NASA STI Program
  Mail Stop 148
  NASA Langley Research Center
  Hampton, VA 23681-2199

NASA/TM-20210021120 AIAA–2021–2649

Isokinetic Probe Total Water Content Measurements in the NASA Icing Research Tunnel With Supercooled Large Drop Conditions

Thomas P. Ratvasky
Glenn Research Center, Cleveland, Ohio

J. Walter Strapp
Met Analytics, Inc., Aurora, Ontario, Canada

Lyle E. Lilie
Science Engineering Assoc., Tolland, Connecticut

Prepared for the
2021 Aviation Forum and Exhibition
sponsored by the American Institute of Aeronautics and Astronautics
Virtual Event, August 2–6, 2021

National Aeronautics and
Space Administration

Glenn Research Center
Cleveland, Ohio 44135

November 2021

Acknowledgments

The authors would like to thank NASA's Aerosciences Evaluation and Test Capabilities project, NRC Canada, Environment and Climate Change Canada, CIRA, and FAA for supporting the SLD Icing Instrumentation Collaboration. Special appreciation is given to the IRT Calibration Team: Judy Van Zante, Laura King-Steen, and Emily Timko for their support in developing the IRT test conditions and for providing their insight in the IRT calibration procedures, and to the IRT technical staff who made these tests happen.

Level of Review: This material has been technically reviewed by technical management.

Available from

NASA STI Program
Mail Stop 148
NASA Langley Research Center
Hampton, VA 23681-2199

National Technical Information Service
5285 Port Royal Road
Springfield, VA 22161
703-605-6000

This report is available in electronic form at http://www.sti.nasa.gov/ and http://ntrs.nasa.gov/

Isokinetic Probe Total Water Content Measurements in the NASA Icing Research Tunnel With Supercooled Large Drop Conditions

Thomas P. Ratvasky
National Aeronautics and Space Administration
Glenn Research Center
Cleveland, Ohio 44135

J. Walter Strapp
Met Analytics, Inc.
Aurora, Ontario, L4G 4Y1, Canada

Lyle E. Lilie
Science Engineering Assoc.
Tolland, Connecticut 06084

Abstract

An Isokinetic Total Water Content Evaporator (IKP2) was used to measure liquid water content (LWC) in the NASA Icing Research Tunnel (IRT) with spray conditions that ranged in LWC and cloud drop size spectra as characterized by the median volumetric diameter (MVD). The IKP2 measurements were made as part of an international collaborative effort to investigate the measurement of supercooled large drop (SLD) conditions in several icing wind tunnels. This report focuses on the IKP2 and background water vapor (BWV) measurements made within the NASA IRT during the October 2017 test entry. The IKP2 LWC results are compared to the IRT LWC calibration values for a range of LWC and MVD values. The IRT LWC calibration is based on measurements from a multi-element hot-wire probe. In general, the IKP2 LWC values were approximately 9 percent greater than the IRT LWC calibration values over a range of LWC from 0.4 to 3.0 g/m^3. The ratio of IKP2 LWC to IRT LWC calibration ranged from approximately 0.9 to 1.27 over a range of MVD from 15 to 460 μm. Comparisons of this data set to IKP2 data from a 2014 IRT test entry show similar results in the regions where overlaps occurred. The results support the theory and observations of water mass loss from hot-wire TWC sensors when subjected to large MVD conditions.

Nomenclature

AIWT	Altitude Icing Wind Tunnel
BWV	background water vapor
CDP	Cloud Droplet Probe (DMT)
CIRA	Centro Italiano Ricerche Aerospaziali
DMT	Droplet Measurement Technologies, Inc.
ECCC	Environment and Climate Change Canada
ICD	ice crystal detector
IKF	isokinetic factor
IKP2	isokinetic total water content evaporator probe, second generation
IRT	Icing Research Tunnel

LWC	liquid water content
MVD	median volumetric diameter
MW	multi-element water content probe (SEA)
NASA	National Aeronautics and Space Administration
NRCC	National Research Council Canada
$\omega_{ambient}$	mass mixing ratio of ambient water vapor (mass of water per mass of dry air)
ω_T	total mass mixing ratio of ambient water vapor + water vapor contained in hydrometeors (mass of water per mass of dry air)
OAP	Optical Array Probe
PSD	particle size distribution
$\rho_{ambient}$	density of air with water vapor
SEA	Science Engineering Associates
SLD	supercooled large drop
SPEC	Stratton Park Engineering Co.
TAT	total air temperature
TWC	total water content

1.0 Introduction

In the early 2000s and again in 2010, international collaborative efforts were performed to understand the state of the art of liquid water content (LWC) and cloud particle spectra measurements of supercooled large droplet (SLD) conditions in icing wind tunnels. Tests were conducted to enable comparisons of legacy and new technology instruments for a range of LWC and median volumetric diameter (MVD) clouds to understand instrument saturation, roll off limits, and other potential limitations when these instruments were subject to SLD conditions (Refs. 1, 2, and 3). As a part of this effort, NASA Glenn researchers anticipated the uncertainties involved in measuring large-MVD conditions with hot-wires due to issues such as splashing and re-entrainment of droplets impacting the wire (Refs. 4 and 5). NASA collaborated with Cranfield University in exploration of a different LWC measurement system that isokinetically ingested cloud droplets into an inlet and evaporator, and then estimated LWC by differencing the humidity in the evaporator flow path to the ambient humidity (Refs. 4 and 6). Similar early developments by the atmospheric science community using this technique have been described in (Ref. 7). Due to the subsequent community interest in high ice water content (HIWC) measurement of natural clouds, the National Research Council Canada (NRCC), Environment and Climate Change Canada (ECCC), NASA, the Federal Aviation Administration (FAA) and Science Engineering Associates (SEA) commenced the development of an airborne isokinetic probe (IKP). The development of the prototype IKP was first described in Reference 8, and the necessary downsizing to the IKP2 for airborne use was described in References 9 and 10. Two copies of the IKP2 were manufactured by SEA, with certain components designed and fabricated by NRCC. It is this instrument, IKP2 serial number 2, which is the subject of this report. Similar instruments have been developed over approximately the same timeframe for use in other icing tunnels (Refs. 11 and 12).

The advent of new icing certification rules for SLD in 2014 (Ref. 13) and the continued uncertainty in particle size distribution (PSD) and LWC measurements in SLD conditions created a need for improvements in instrumentation and data analysis processes that required assessment and validation. This need motivated a new international collaboration between Centro Italiano Ricerche Aerospaziali (CIRA), NASA, FAA, NRCC, ECCC, and Met Analytics, Inc. In 2015, these organizations along with

probe manufacturers Artium and Science Engineering Associates (SEA) initiated the development of a common set of test plans to assess various water content and particle sizing instruments at the NRCC Altitude Icing Wind Tunnel (AIWT), the NASA Icing Research Tunnel (IRT) and the CIRA Icing Wind Tunnel (IWT) (Ref. 14).

The first test entry of this collaborative effort at the NASA IRT was in October 2017. The drop sizing instruments that were tested included the Droplet Measurement Technologies (DMT) Cloud Droplet Probe (CDP2), Stratton Park Engineering Co (SPEC) 2D-S, the Artium Phase Doppler Interferometer (PDI), and the Artium High Speed Imager (HSI). The water content instruments that were tested included the SEA multi-element water content probe (also known as 'multiwire', or MW) (Refs. 15 and 16), the SEA Ice Crystal Detector (ICD) (Ref. 17), and the isokinetic evaporator probe (IKP2) (Refs. 9 and 10).

The purpose of this report is to compare the results of the IKP2 LWC measurements to the IRT calibrated LWC values (hereafter the IRT LWC_cal) over a range of cloud LWC and MVD conditions, and discuss potential reasons for differences found through this investigation.

2.0 Experimental Description

The IKP2 was installed at the centerline of the IRT test section (Figure 1). Background water vapor (BWV), necessary for IKP2 LWC calculation, was measured at two locations. One BWV inlet was on the side of the IKP2 canister (Figure 2), while the second BWV came from an aft facing inlet on a tube mounted to the IRT ceiling (Figure 3). The air sampled by each BWV inlets flowed through approximately 12 ft of 0.25 in. outer diameter Teflon tubing to Licor LI840A H_2O gas analyzers that were located above the IRT test section (Figure 4). The vertical tube for BWV2 was extended into the IRT to various vertical positions. An SEA MW probe (s/n 2023, the IRT primary calibration probe) was also mounted about 15.5 in. off horizontal centerline (toward the north side of the IRT), but the sensor was at vertical centerline. Based on a review of IRT LWC uniformity contours (Ref. 18), the cloud at this location was within 80 to 100 percent of the centerline LWC values for small and large MVD cloud conditions. The SEA MW probe at this location was used as a real-time reference for the IKP2 data. The IKP2 inlet was approximately 16 in. forward of the SEA MW probe.

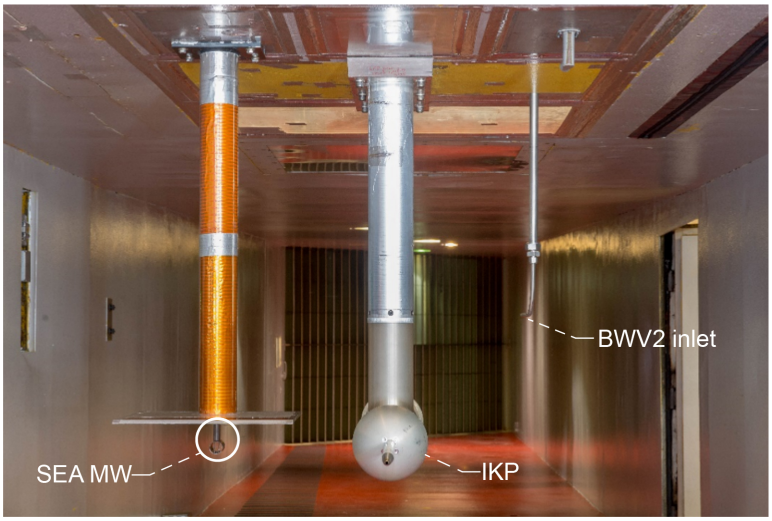

Figure 1.—General setup with IKP2 at primary centerline position.

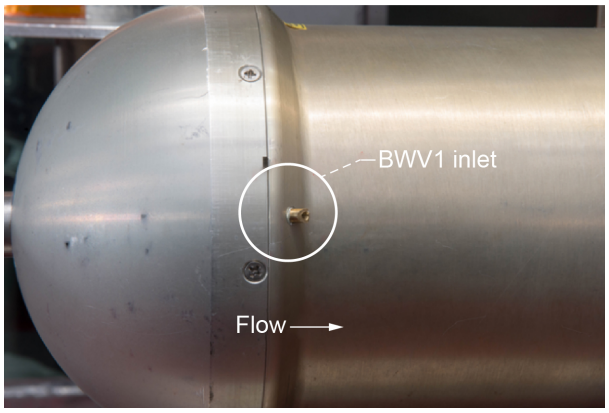

Figure 2.—BWV1 inlet (~ 3.5 in. left of centerline).

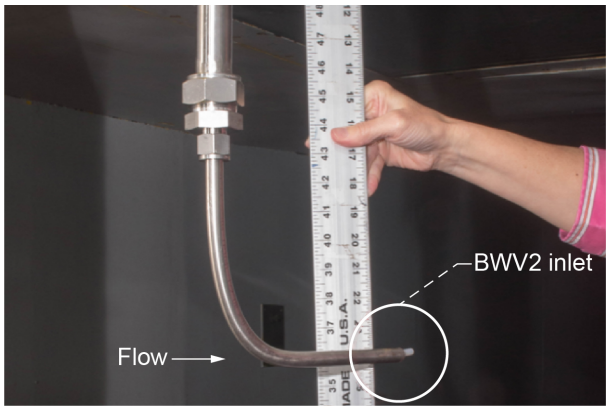

Figure 3.—BWV2 inlet (~16 in. left of centerline and 12 in. above centerline).

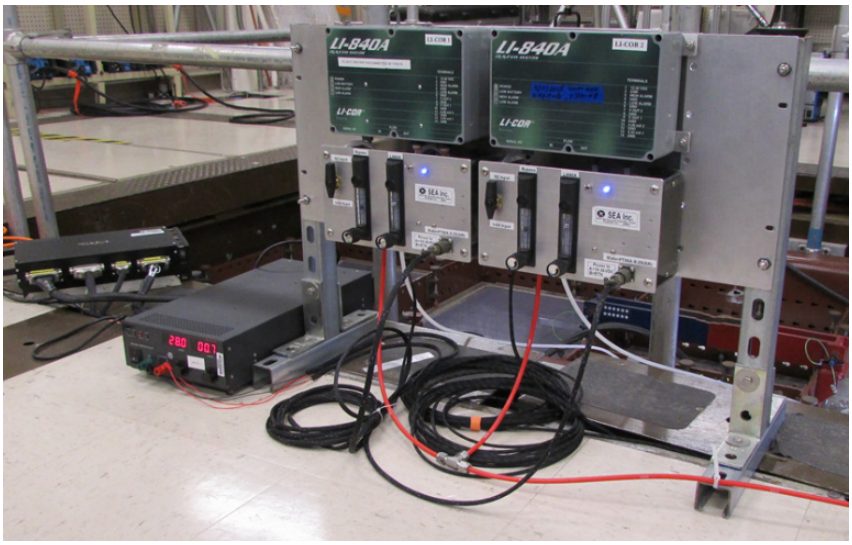

Figure 4.—Background Water Vapor Measurement System.

Prior to this IRT test, all LI840A H_2O gas analyzers were recalibrated at Licor, and the IKP2 was calibrated using a customized cart that injected precise water flow rates at the inlet and induced airflow through the IKP2 using vacuum at the IKP flowpath exit/vent. Figure 5 provides the results from that calibration and shows the IKP2 measured values were within nearly 2 percent of the injected water contents between 1 to 33 g/m^3. Further description of this calibration method is given in Reference 9.

The test matrix for the IKP2 is shown in Table 1 and consisted of 35 sprays. The LWC and MVD for each spray were determined through previous IRT calibrations (Ref. 18). The IRT LWC_cal is based on centerline measurements with a SEA MW, and the IRT MVD_cal is based on centerline measurements with a DMT CDP, and two Optical Array Probes (OAP-230X, and an OAP-230Y) (Ref. 18).

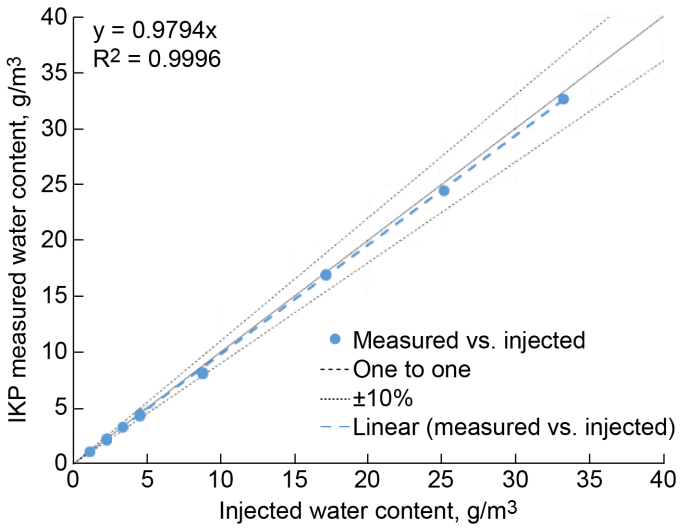

Figure 5.—IKP2 calibration results prior to IRT Test.

TABLE 1.—TEST MATRIX USED IN THE IKP2 TESTING ON OCTOBER 18, 2017

Description	Velocity, m/s	IRT MVD, μm	IRT LWC, g/m^3	TAT, °C
LWC Sweep (small MVD)	77	20	0.4 to 3.0	–10
MVD Sweep (moderate LWC)	77	15 to 460	0.4 to 1.4	–10
LWC Sweep (large MVD)	77	138	0.4 to 0.9	–10
LWC Sweep (small MVD, high speed)	129	20	0.6 to 1.2	–10

3.0 Data Processing and Analysis

The IKP2 data analysis starts with processing the Licor LI840A gas analyzer data (one unit is internal to the IKP2 and two are external for the BWV1 and BWV2) into time histories sampled at 1-s intervals for each spray. These data are then set to a common prespray value to manage small offsets that may occur with the three individual instruments. In this analysis, the common prespray value was set to a water vapor value derived from an independent Vaisala Relative Humidity instrument mounted at the IRT spray bars. By doing this, two assumptions are made: 1) that no significant water vapor mass is added through evaporation or sublimation processes, or subtracted through condensation or riming processes as air moves from the spray bars to the test section during the prespray reference point, and 2) the water vapor is uniformly distributed throughout the tunnel cross-section where the sensor or inlets are located. During these tests, no prespray condensation clouds were observed in the test section. The offsets of the IKP2, BWV1 and BWV2 Li840A units from the calculated Vaisala RH instrument were on average –35, 186, and 146 ppm respectively with standard deviations of approximately 40 ppm, and were considered acceptable based on the authors' experience with these units. The IKP2 TWC values are determined using Equation (1) by calculating the total mass mixing ratio from the IKP2 Licor (ambient water vapor + water vapor from evaporated hydrometeors that enter the IKP2 inlet) and subtracting the mass mixing ratio from the ambient air (sourced from the BWV Licors) and then performing the remaining calculations in Equation (1), from (Ref. 10). The isokinetic factor (IKF) is a multiplier to compensate for flow path humidity effects when the measured mass flow rate through the IKP2 is not

equal to the desired isokinetic mass flow rate. This correction factor is straightforward for ballistic sizes (diameter > 100 μm), but becomes less accurate for large departures from unity and/or small droplet sizes. The IKF values calculated for the results presented hereafter ranged from 0.97 to 1.04, but were within 0.98 to 1.02 for most test points. For more background on the IKP2 calculations and performance, see References 9 and 10. Since two BWV were available, results of two IKP2 TWC calculations will be presented.

$$\mathrm{TWC} = \left[\frac{\omega_T - \omega_{\mathrm{ambient}}}{(1+\omega_{\mathrm{ambient}})} * \rho_{\mathrm{ambient}} * 1000\right] * \mathrm{IKF} \quad (1)$$

where
ω_T = total mass mixing ratio of ambient water vapor + water vapor evaporated from hydrometeors
$\omega_{ambient}$ = mass mixing ratio of ambient water vapor
$\rho_{ambient}$ = air density with ambient water vapor
IKF = Isokinetic Factor = measured mass flow rate / isokinetic mass flow rate

The following three figures are examples of the analysis that highlight specific observations. Figure 6 shows results from a low LWC and small MVD test point (IRT-21c: LWC = 0.42 g/m^3, MVD = 14.9 μm). The top panel of Figure 6 shows the time histories of the water vapor (WV) values from the IKP2, and the two BWV inlets. The middle panel provides a closer examination of the WV from the two BWV inlets as well as the calculated water saturation. The bottom panel shows the time histories of LWC values from the IKP2 based on both BWVs, the real-time MW, and the IRT calculated LWC based on spray nozzle parameters using the 2015 IRT calibration curves. Although the legend in these figures indicate IKPTWC, the IRT spray conditions tested were all liquid, and therefore the IKPTWC results are considered to be a measure of LWC.

Reviewing the upper panel, note that WV values were normalized as described above for the pre-spray timeframe. Any lags in the BWV data due to transport time from inlet to Licor sensor were time-synchronized as well. In this test, these lags were typically 1 s. From the upper and middle panel of Figure 6, shortly after the spray cloud was initiated (Spray On = 1), WV values increased for the IKP2 and both BWV measurements. During the spray, the BWV2 (purple line) rose to very close to the calculated water saturation level (light blue line). The BWV1 (green line) measured about 60 ppm higher WV value than BWV2. About 45 s after Spray Off, all WV values returned to the pre-spray values. This indicates no significant contamination in the BWV inlets and little recirculation in the tunnel. Had there been significant contamination in the BWV inlet, the measured value would have been positively offset from the IKP WV value after the Spray Off. If there had been recirculation in the tunnel, the time to return to pre-spray values would exceed the 45 s shown in this case. The WV data was converted into LWC based on Equation (1) and these results are shown in the lower panel for the IKPTWC_BWV1 (green) and IKPTWC_BWV2 (purple). The real-time MW_TWC data with correction for collision efficiency based on (Ref. 19) is shown in the pink trace and the IRT_LWC_Calc (orange trace) shows the real-time calculation of LWC based on the 2015 IRT calibration fit for the spray bar and tunnel airspeed values. The Spray On time is indicated by the black dotted line shifting from 0 to 1 based on right hand vertical axis. This figure is an example of typical results for lower LWC and smaller MVD clouds. For the summary plots shown in Section 4.0, Results, 2-min average values were derived for the LWC data shown between the two dotted blue vertical lines on this plot.

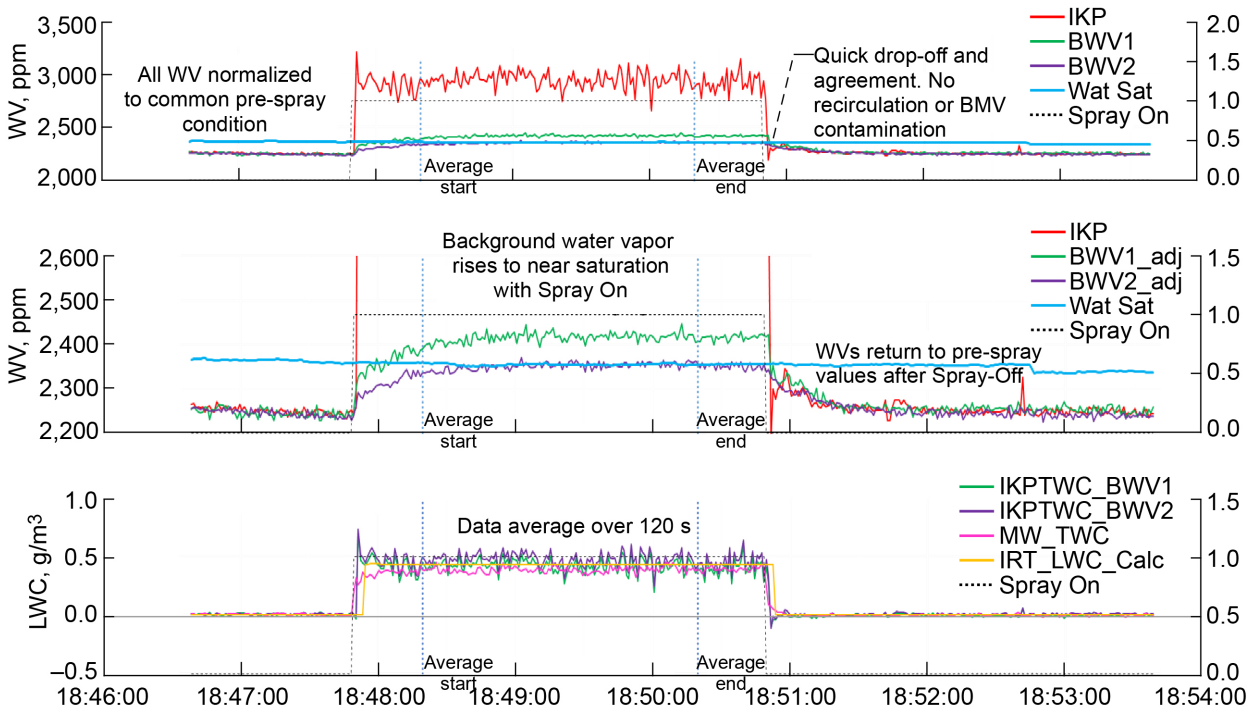

Figure 6.—Time history of WV and derived LWC for low LWC and small MVD spray condition.

Figure 7 shows results from a high LWC and small MVD test point (IRT-5: LWC = 2.47 g/m^3, MVD = 20.7μm). In this example, note in the upper panel the large difference between the IKP WV and the BWVs—this signifies more water content in the cloud. The middle panel shows after Spray-On, both BWV exceeded the calculated water saturation level by about 8 percent. Water saturation was calculated using the calculated static temperature and measured static pressure in the test section. This calculation is highly sensitive to temperature; a +0.5 °C error in the static air temperature for this test condition could raise the water saturation level by 4 percent. Consequently, the calculated saturation level could be less than actual water saturation due to a small increase in local static temperature. A possible cause for such a temperature rise in the test section is an exchange of heat from spray water to air as the larger volumes of spray water were supercooling. Alternatively, the air may have been super-saturated to some level due to the rapid change of temperature and pressure without sufficient time for all excess water vapor to condense on existing droplets. This potential for super-saturation was discussed in Reference 20 for icing tests in the NASA Propulsion System Laboratory. At Spray-Off, all WV values reduced immediately to near the calculated saturation level for about 15 s, which indicates a condensation cloud may have been present in the test section, although no notes of such clouds were made. After the 15 s passed, all WV values reduced consistently, which indicated no significant water contamination in the BWV lines. Note in the bottom panel that the real-time MW did not show a significant LWC measurement immediately after Spray Off.

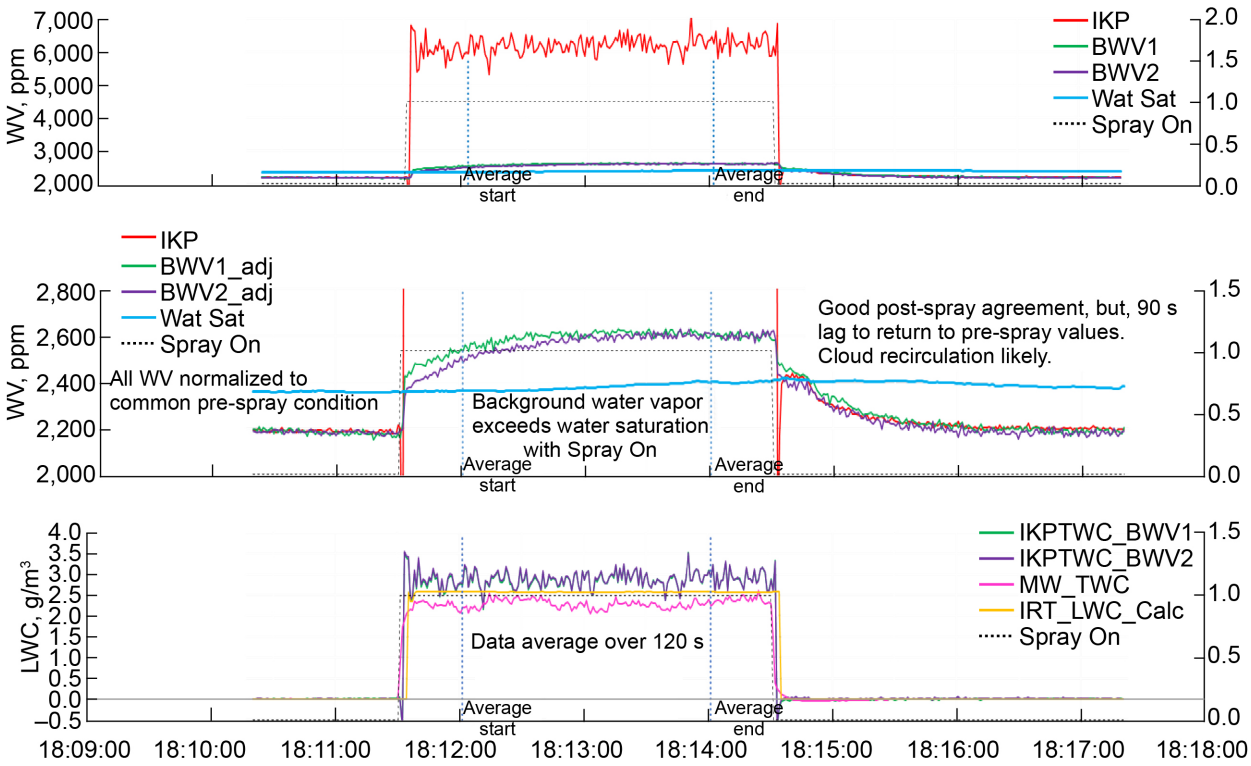

Figure 7.—Time history of WV and derived LWC for high LWC and small MVD spray condition.

Figure 8 shows results from a moderate LWC and large MVD test point (IRT-29: LWC = 1.36 g/m^3, MVD = 460 μm). As in the previous examples, the upper panel of Figure 8 shows the WV were normalized and time-synchronized before Spray-On and after Spray-Off, all WV values quickly returned to the pre-spray values indicating no significant BWV line contamination or cloud recirculation. However, during the Spray-On, the rather large variations in IKP2 WV values are noteworthy. The authors propose these variations are caused in part by the pulses of water vapor after the larger size drops are evaporated. These larger variations are also possibly amplified by an overshoot/undershoot problem that was discovered with the Licor LI840A units when very large step changes occurred (Ref. 21), such as when a spray is turned on or off (e.g., see start and end of spray in Figure 6). It was found in (Ref. 21) that the effect of the overshoot/undershoots are minimized when applying a 5-s or longer moving-average. The bottom panel of Figure 8 shows the LWC results with a 5-s moving-average to demonstrate this. These overshoots/undershoots had negligible effects on the 2-min averages presented in this article.

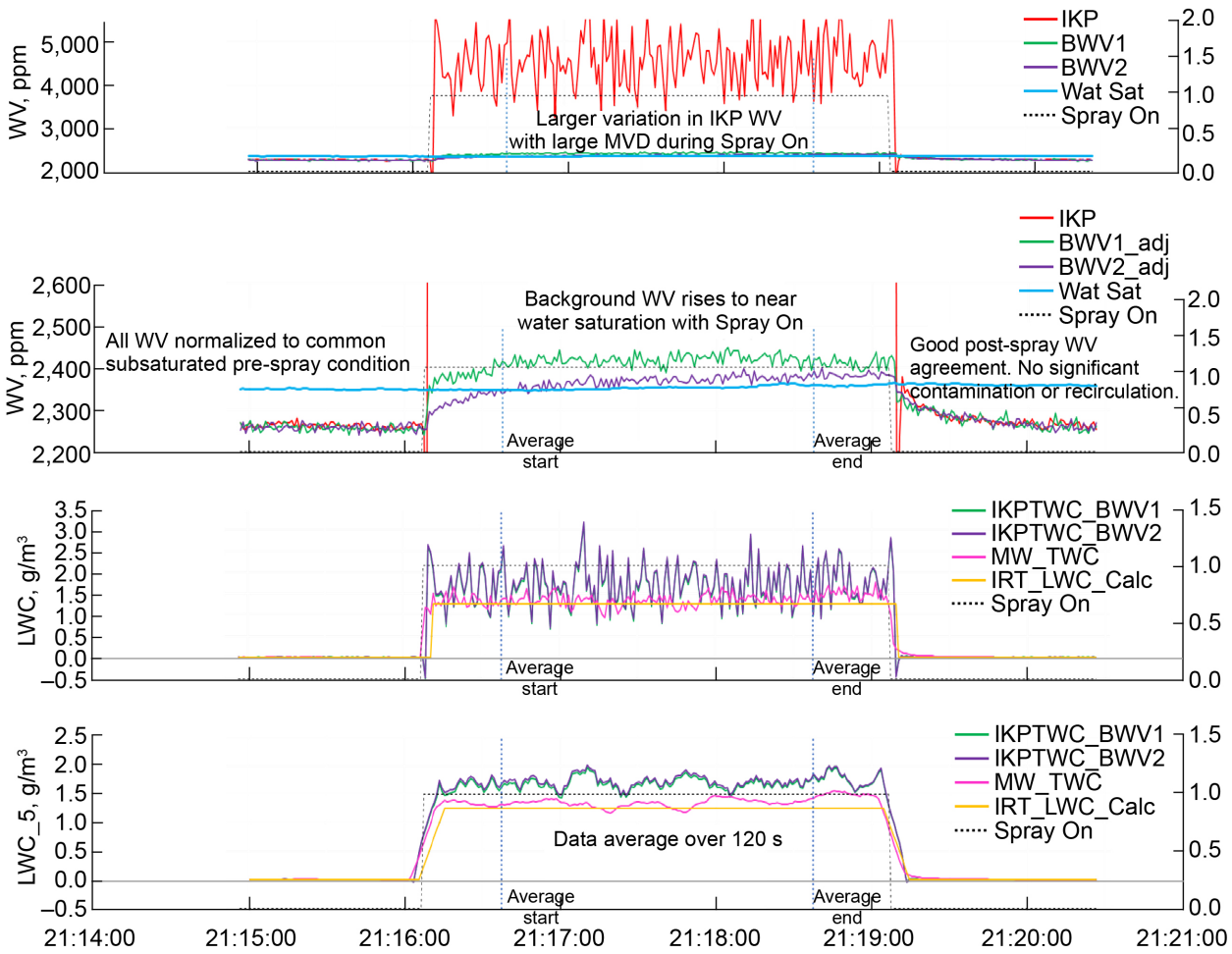

Figure 8.—Time history of WV and derived LWC for moderate LWC and large MVD spray condition. Bottom panel shows LWC values with a 5-s moving average.

4.0 Results

Each of the 35 IRT sprays was analyzed as described in the previous section, where the 1-s TWC data shown in the time histories was averaged over 120 s during a steady portion of the Spray-On periods. Since the IRT spray water and air were heated as normal, the spray cloud is assumed to be composed of liquid drops only, so the IKP2 TWC measurements represent the LWC in the cloud.

4.1 IKP2 Response Over a Range of LWCs

One objective in the SLD icing instrumentation testing is to document the instrument response over a range of LWC conditions. The time-averaged IKP2 TWC values from the LWC sweeps, plotted versus the IRT calibrated LWC values, are shown in Figure 9. In this and subsequent figures, the green circles represent the IKP2 TWC based on the background water vapor from the BWV1 inlet on the side of the IKP2 canister. The purple triangles represent the IKP2 TWC based on the background water vapor from the BWV2 inlet that was downstream and about 16 in. left and typically 12 in. above centerline. Note these data represent LWC sweeps with MVD points ranging 14 to 460 μm and airspeeds at 77 and 129 m/s.

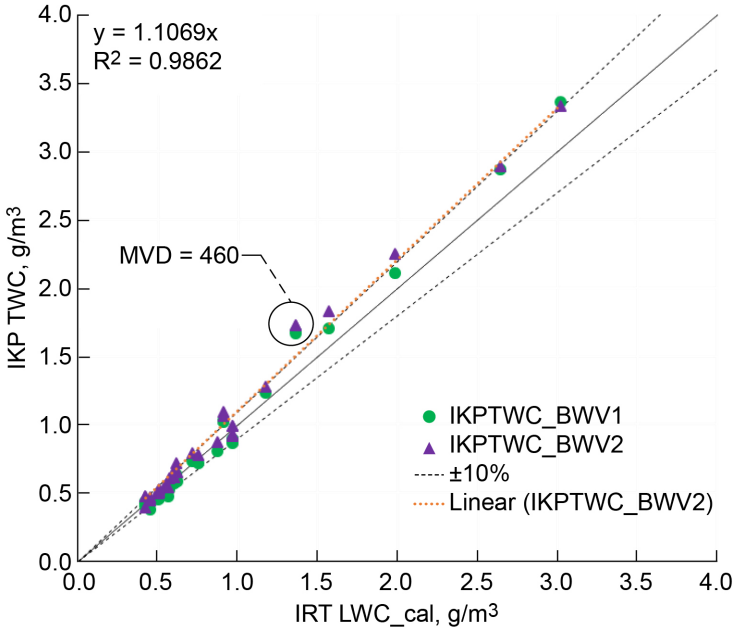

Figure 9.—IKP TWC to IRT calibration LWC for all MVD and airspeeds.

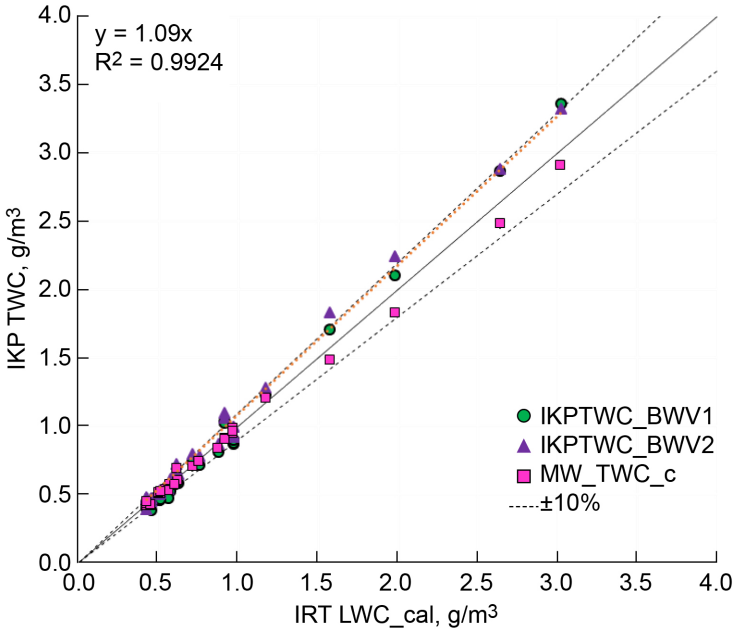

Figure 10.—IKP and MW TWC to IRT calibration LWC for all MVD and airspeeds with MVD 460 removed.

The IKP2 TWC based on BWV1 was on average about 8 percent lower than the IKP2 TWC based on BWV2 for IRT LWC_cal up to 2 g/m^3. For higher IRT LWC values, the IKP2 TWC was nearly the same regardless of the BWV source. This is consistent with the BWV traces shown in Figure 6 and Figure 7 where the BWV1 values were greater than the BWV2 values. When the greater BWV1 value is subtracted from the IKP2 BWV value, it results in a lower TWC. This observation will be further developed in Section 5.0, Discussion.

Also noted on Figure 9 is a linear regression trend line with the offset forced to 0 for the TWC_BWV2. The slope of this line shows the TWC_BWV2 is about 10 percent greater than the IRT LWC_cal values. This result included the MVD = 460 μm test point, which deviates most from the rest of the data set.

Figure 10 shows the same results as Figure 9, but with the MVD = 460 μm test point removed. The rationale for doing this will be included in Section 5.0, Discussion. The removal improved the agreement of the IKP2 TWC to be 9 percent greater than the IRT LWC_cal as shown in the linear fit and R^2 values. Figure 10 also shows the values from the TWC element of the SEA MW probe (pink squares) that was adjacent to the IKP2 during these sprays and provided a run-time reference. The best fit lines between the IKP2 and IRT LWC_cal values are remarkably similar to the corresponding 2014 results of Reference 9, where it was shown that the slope of the linear regression of the IKP to IRT LWC_cal was 1.102 for the same IKP2 serial no. 2.

4.2 IKP Response Over a Range of MVDs

Another objective in this test was to document the instrument response over a range of small to large MVDs. One way to compare the IKP2 TWC results to the IRT LWC_cal results is to look at the ratio of these two over the range of MVDs. Figure 11 shows this ratio of IKP2 TWC/IRT LWC_cal and MW_TWC/IRT LWC_cal for IRT MVD_cal points ranging from 14 to 460 μm. Ideally, the LWCs for the MVD sweeps would have been constant. However, to reduce uncertainty in the LWC and MVD values, the test points were limited to measured spray conditions used in prior IRT calibrations. Most test points in the MVD sweep had IRT LWC_cal values were near 0.5 g/m^3, but for the larger MVDs, the IRT LWC_cal increased up to 1.36 g/m^3.

At the very lowest MVD point, the IKP2 TWC_BWV2/IRT LWC_cal (purple triangle) is approximately 1.13, but moving to moderate MVDs, the ratio values decrease and are within the 10 percent band up to MVD's near 200 μm. For MVDs 200 to 460 μm, the ratio increases from 1.1 to 1.27. The IKP2 TWC_BWV2 values are consistently greater than the IKP2 TWC_BWV1 (green circles)

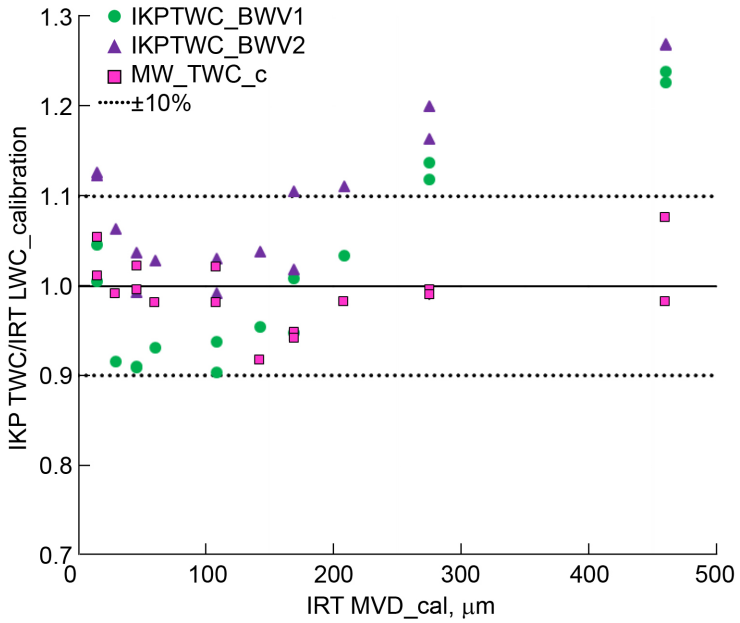

Figure 11.—Ratio of IKP and MW TWC to IRT LWC_cal for a range of IRT MVD.

as stated earlier, but these points also show ratios greater than 1.1 for MVDs 275 to 460 μm. The ratio using real-time MW results (pink squares) are all within the ±10 percent band which indicates the spray cloud was consistent with the IRT calibration values throughout the MVD sweep. This result was expected since the IRT LWC_cal was established using the MW TWC sensor.

5.0 Discussion

5.1 Background Water Vapor Differences

The measurement of BWV in the cloud has proven to be a challenging problem. Experience during flight campaigns has shown that BWV inlets can be subject to water or ice contamination in clouds for a variety of reasons (Refs. 9 and 21). Reference 22 indicated that phase relaxation times in liquid clouds can range from 2 to 40 s. In the IRT, the time for droplets to travel from spray bars to test section is on the order of 2 to 3 s for the airspeeds used in this test. The reductions in static temperature and pressure that occur due to wind tunnel wall geometry changes between the spray bars and the test section are significantly faster than the temperature and pressure changes that occur in natural clouds. Consequently, certain thermodynamic equilibria present in natural clouds, such as water-saturation when in significant LWC, cannot necessarily be assumed as reference points in icing wind tunnel clouds. At sea level pressure and static temperatures of (0, –10, –20, and –30 °C), the water-saturation BWV levels are approximately (4.86, 2.35, 1.07, and 0.45 g/m^3), respectively. At these conditions, the subtracted BWV term can be as high or higher than the LWC to be calculated, and special care is required, such as the normalization procedure outlined in Section 3.0, in order to provide optimal IKP2 LWC results. In typical tunnel experiments, although the BWV levels are relatively high, they are fortunately also quite stable.

As was shown in Figure 6 and Figure 7, the background water vapor measured during the Spray-On periods by the inlet on the side of the IKP2 canister (BWV1) was typically higher than the background water vapor measured at the stand-alone reverse flow inlet (BWV2). The maximum difference (Δ BWV) was 174 ppm (equates to 0.14 g/m^3 for this test condition) for the LWC = 2 g/m^3 point during the LWC sweep with MVD = 20 μm, and the average BWV difference from all test points was 74 ppm (0.06 g/m^3). The differences for all the test points is shown in Figure 12, but no systematic trend was determined.

With the BWV1 inlet on the side of the IKP2 canister, there was speculation that there could be additional water vapor in the boundary layer air near the IKP2 canister caused by water evaporating on the heated IKP2 inlet. During one of the IRT test points, this potential effect was examined by initiating a spray as normal, then turning off the IKP2 inlet heat and allowing the inlet to cool and ice up, then turning the inlet heat back on. The data from this test are shown in Figure 13. After Spray-On, there was a step change in the water vapor on the IKP2 and both BWVs. The IKP2 tip heat was turned off after about 15 s and after about 45 s, the measured mass flow through the IKP2 went to 0 kg/s, indicating the tip was iced over. At that time, the BWV1 was about 115 ppm higher than BWV2. After the IKP inlet heat was turned on, the BWV differences remained fairly constant, even though the cloud was still on. From this observation, the test team determined that the IKP2 inlet heat did not increase the water vapor sensed by the inlet on the side of the IKP2 canister. A side note should be made regarding the decreasing WV on BWV2 prior to Spray-On in this figure. Early in this IRT test, the BWV2 inlet became contaminated with water, so the measured values were positively offset. However, the measured BWV2 values were decreasing due to the air line drying out over time in subsaturated air. The pre-spray normalization fixes the offset, but does not account for the reduction as the air line dries. This was accounted for in the post processing during the Spray-On, but this figure shows the deviation for pre-spray BWV2 time history.

Other speculations regarding the BWV differences observed are:

- Could there be a stratification of the BWV in the IRT test section when the cloud was turned on? This would imply that portions or all of the IRT cloud are subsaturated with respect to water.
- Could the relatively large dome on the IKP2 be a source for additional water vapor in the boundary layer air (near BWV1 inlet) as water drops impact, emit latent heat of fusion as water transitions to ice, enabling more WV to be absorbed in the air?
- Could BWV1 be more likely to entrain water droplets into its inlet, or evaporate droplets in the vicinity of the inlet due to adiabatic compression and local temperature increase?

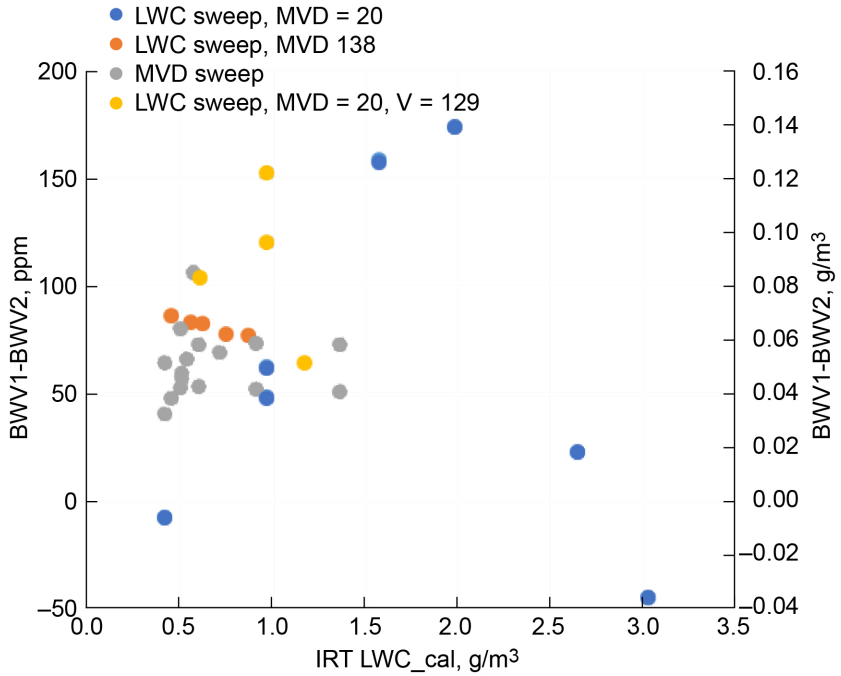

Figure 12.—BWV differences versus IRT LWC_cal.

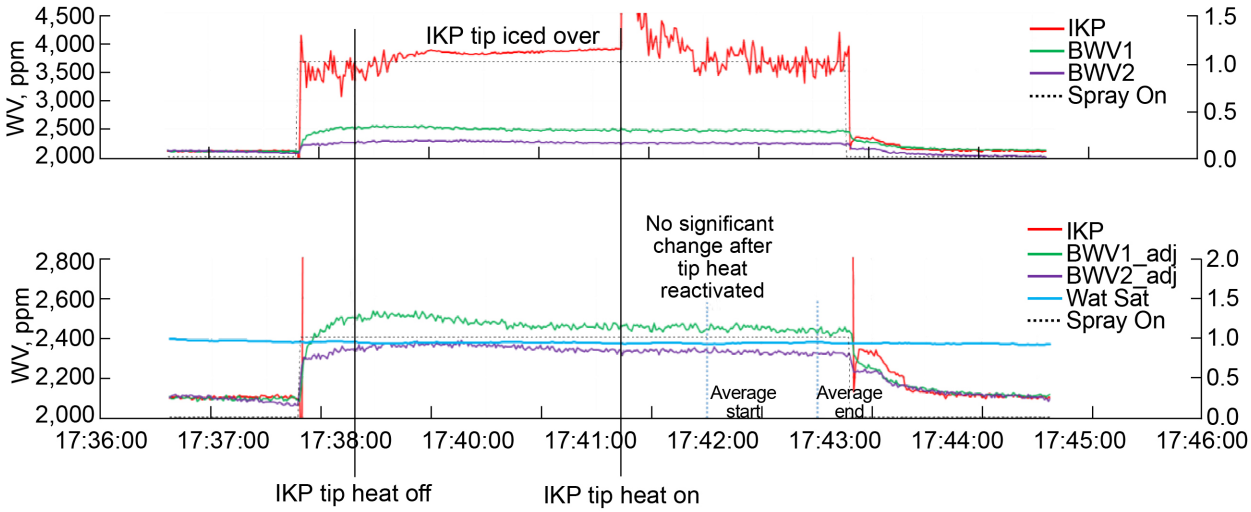

Figure 13.—Time history showing background water vapor changes with IKP2 inlet heat.

During this IRT test, some testing on BWV stratification in the IRT was examined using the BWV2 inlet, which was inserted into the tunnel at different offset positions from 0 to 24 in. above centerline. The run time review of the BWV2 data found no significant changes in the data from these different vertical positions, so most of the BWV2 data was mostly collected at 12 in. above centerline. A more thorough test of the BWV sensitivity to inlet position is warranted. Likewise, more analysis is needed to understand if ice formation on the IKP2 dome could be a source for additional water vapor in the boundary air near the BWV1 inlet.

In summary, both BWV1 and BWV2 rose during liquid sprays, either due to contamination or due to true rises in the BWV. BWV1 generally rose higher than BWV2, either due to more contamination, or due to local gradients in BWV within the IRT cloud, or some other factor. Comparisons of the BWVs immediately post-spray to the IKP2 value, assumed to be insensitive to contamination, suggested that neither BWV1 nor BWV2 suffered from significant contamination that would require multiple tens of seconds or more to clear. Speculation of local drop evaporation due to adiabatic compression remains as a possible contaminating effect. The magnitude of the in-cloud BWV1-BWV2 difference reached about 0.14 g/m^3 at a LWC of 2 g/m^3 and an MVD of 20 μm. The solution to the question as to which BWV is correct, if either, is complex and unresolved. Unpublished flight campaign measurements by the authors on the NASA DC-8 using BWV1 and a similar inlet to BWV2, albeit at much higher airspeeds and lower temperatures, strongly suggested BWV contamination occurred in glaciated clouds. Further testing of BWV accuracy using inlets is warranted to optimize IKP2 LWC estimates. Experiments could include more thorough testing of BWV sensitivity to inlet position within the cloud, and more study on the effect of ice accretion on the IKP2 dome. The uncertainty in IKP TWC can be reduced by testing at colder temperatures, where BWV is much lower and therefore has less impact on the IKP2 TWC calculation.

One last discussion item on the BWV and its impact on IKP TWC calculations is considered. The calculated TWC using the IKP2 can be greater than the actual LWC in the cloud if one or both of the following occurs:

- The mass flow through the IKP inlet is lower than the measured mass flow. In this scenario, the mass from all but very small drops would be captured in the inlet, but with less air mass. This would result in an elevated IKP WV value. Prior to the IRT testing, the mass flow through the IKP2 was measured and checked during tests with the IKP2 calibration cart. During the IRT testing, the mass flow through the IKP2 is regulated to maintain an IKF near unity. For these tests, the IKF ranged from 0.97 to 1.04, and this IKF correction was applied to all IKP TWC calculations to account for these small deviations.
- The measured BWV is less that the actual BWV in the cloud. This will result in an elevated TWC since the BWV is subtracted from the IKP WV to derive the TWC. The potential issues with the BWV inlets described above (entrainment of water droplet into the inlet or rise in local temperature near inlet) would cause the BWV to be over-estimated, rather than underestimated. Therefore, these issues that drive uncertainties in BWV would lead to lower TWC calculation rather than higher TWC calculations.

5.2 Variations in Ratio of IKP2 TWC/IRT LWC_Cal at Small and Large MVDs

The IKP2 TWC_BWV2/IRT LWC_cal ratio data from Figure 11 was replotted in Figure 14 and a hand-drawn line was added to show a trend that was observed in this data. At the smallest MVD = 14 μm test point, the IKP2 LWC is about 13 percent above the IRT LWC_cal values. As MVD increases, the agreement between the IKP2 and IRT LWC_cal improves so that at the MVDs between 45 to 130 μm, these

measurements are within 4 percent of one another. As the MVD increases from 170 to 460 μm, the ratio of IKP2 TWC to IRT LWC_cal increases from about 1.05 to 1.27. Although not shown on Figure 14, a similar trend was observed with the IKP2 TWC_BWV1 values. Potential reasons for this observed trend follows.

Rigby et al. (Ref. 19) calculated collection efficiencies for the MW elements for drop sizes 5, 20, 50, and 100 μm at two airspeeds and two total pressures. The MW TWC element is concave and is sometimes referred to as a half-pipe. Rigby's analysis showed that as drop size decreases, the collection efficiency of the half-pipe also decreases. The half-pipe collection efficiency decreases from 0.93 to 0.70 for drop sizes of 20 and 5 μm, respectively at the lower airspeed case of 85 m/s. Since 2015, corrections for collection efficiency based on Rigby's analysis have been applied to the measured MW LWC in the IRT calibration tests (Ref. 18) and the MW LWC compared well to the icing blade at these lower MVD and LWC conditions (Ref. 23). The collection efficiency correction is a function of airspeed and MVD, but analyses were performed with the full particle size distribution and found correction values were within a few percent using the MVD. For the smallest MVD point tested (MVD = 14.9 μm) and airspeed of 77 m/s, the measured MW TWC data was divided by 0.91 to correct for the lower collection efficiency of the MW concave element.

Perhaps one possible explanation for the higher IKP2 TWC at these smaller MVD test points is that the current corrections for collection efficiency of the MW half pipe are not sufficiently accounting for low collection efficiencies of the small drops in the particle size distribution. Figure 15 is a normalized cumulative volume from a recent IRT calibration using the same nozzle settings as the MVD = 14.9 μm point in Figure 14. Note that about 25 percent of the water volume is in drops less than 10 μm and 10 percent of the water volume is in drops from 4 to 8 μm. The IKP2 measures the water contained in all drop sizes, small and large, while the MW TWC sensor is less efficient in collecting drops 10 μm or less. As stated above, the current collection efficiency correction process using the MVD was compared to the total collection efficiency for a binned size distributions and were within a few percent. Perhaps that difference would bring the IKP measurement closer to the IRT_LWC calibration.

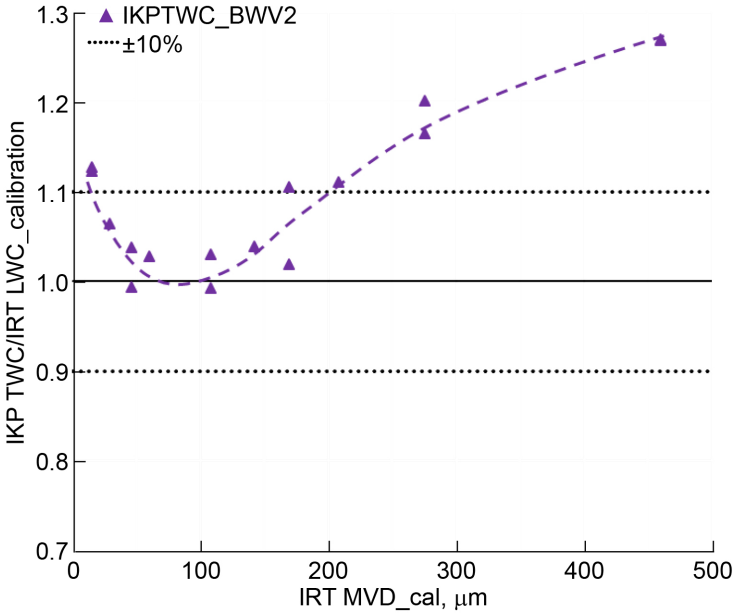

Figure 14.—Trend observation of IKP2 TWC_BWV2 to IRT LWC_cal for a range of IRT MVD.

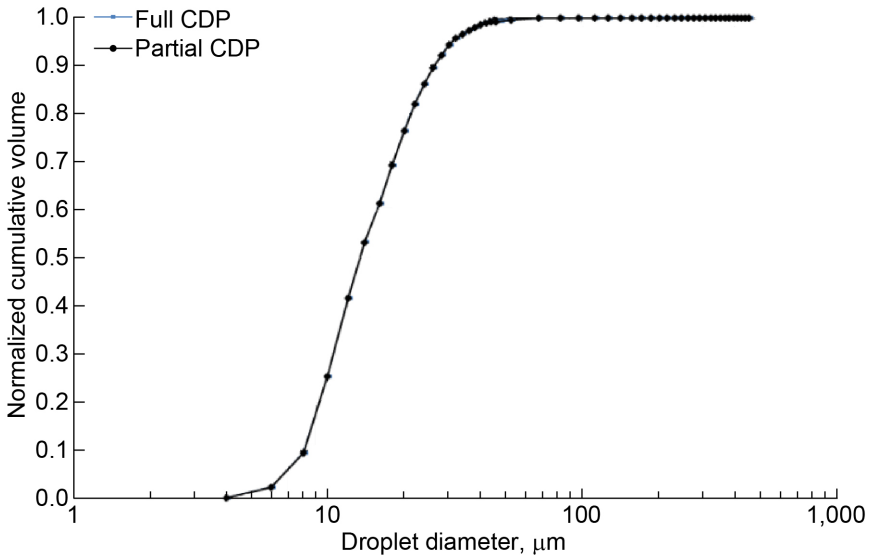

Figure 15.—Normalized cumulative volume vs drop size for IRT calibration, Pair = 20, delP = 25.

Another possible explanation for the higher IKP2 TWC at these smaller MVD test points is a scoop effect at IKFs >1 that draw in proportionally more small water drops than air into the inlet at the low Stokes number conditions. This condition was examined in (Ref. 10) which showed a 5 percent increase in collection efficiency for IKF = 1.05 for very low Stokes number (0.07) conditions, but the collection efficiency at this condition did not exceed 1.0, which would be needed to collect more water than air in the inlet. The IKF for the low MVD conditions shown in Figure 14 was further reviewed and found to be on average 1.000 with a standard deviation of 0.006 during Spray-On times. Although the scoop effect is not likely a cause for the higher IKP2 values in Figure 14, further research on IKP2 inlet catch efficiency and additional confirmation of the mass flow measurements would be valuable.

It is also important to restate the MW and icing blade show good agreement in this low MVD, low LWC icing condition. If the discrepancy between the IKP2 and the IRT LWC cal is due to the water mass contained in very small drops, it is unlikely that these droplets would impinge on typical airfoil models and add significantly to the resulting ice accretion. This concept of "accretable" water was discussed in Reference 6.

The increase in the ratio IKP2 TWC to IRT LWC_cal for MVD's 200 to 460 μm shown in Figure 14 is a key finding of this SLD Icing Instrumentation testing. This increase may in part be due to mass loss of large drops splashing from the MW concave sensor before the impinging water mass was completely evaporated. Observations of impinging mass loss on hot-wire probes were described in Reference 5, and mass loss on hot-wire water content probes in SLD conditions was a primary reason for developing isokinetic probes in the early 2000s (Refs. 4 and 6). Since the IRT LWC_cal value was based on a MW concave sensor that has the potential for mass loss in large MVD and moderate LWC conditions, the MVD = 460 μm test point was removed from Figure 10 in order to develop the trend-line without this outlier. It is noted that additional tests with the IKP2 using MVD sweeps at other fixed LWCs would be beneficial to support or refute this finding of potential mass loss on the hot-wire instruments and possibly enable the development of hot-wire TWC efficiency factors for large MVD cases.

6.0 Summary and Conclusions

As part of the SLD Icing Instrumentation collaborative research, the IKP2 was tested at the NASA IRT in 35 spray conditions where LWC ranged from 0.4 to 3 g/m^3 and MVD ranged from 15 to 460 μm. This report documents specific observations in the IKP2 and BWV measurements under these test conditions. IKP TWCs were calculated using two sources of BWV—an inlet on the IKP2 canister and another in a reverse-facing tube. The inlet on the IKP2 canister consistently measured higher BWV compared to the reverse facing tube, which led to differences of about 8 percent in the calculated TWCs. Speculations are offered on causes for these differences. Although there is some uncertainty in the BWV, this issue is not considered to alter the major conclusions.

The resulting IKP2 TWC values were compared to the IRT LWC calibration measurements in various ways. The IRT LWC calibration is based on measurements of the TWC concave sensor of an SEA MW hot-wire probe. A linear fit of IKP2 TWC to IRT LWC_cal over a LWC range of 0.4 to 3 g/m^3 indicated the IKP2 measured the LWC approximately 9 percent higher than the IRT LWC calibration for MVDs ranging between 15 to 270 μm. These results were in good agreement with test results of the same IKP2 in the IRT from 2014. Additional tests with MVD sweeps and LWC sweeps are needed to better understand potential causes for this difference. If the difference is related to the water mass contained in very small droplets, it is speculated that the LWC difference will not significantly affect the ice shapes on typical airfoil models since very small droplets are unlikely to impinge due to low inertia properties.

The ratio of IKP2 TWC to IRT LWC_cal was also examined over an IRT MVD_cal range of 15 to 460 μm. The IKP2 results were generally higher than, but within +10 percent of the IRT LWC_cal values for MVDs < 200 μm. However, for MVDs > 200 μm, the IKP2 TWC was 10 to 27 percent greater than the IRT LWC_cal. One possible explanation for this finding is the loss of water mass from the MW concave sensor when large drops impinge and splash out of its capture volume. Isokinetic evaporator probes were designed to fully capture small to large size hydrometeors to address this specific issue of mass loss. The IKP2 TWC measured LWC should not be subject to these mass losses, and should generally be expected to provide a more accurate measure of LWC for the large MVD test conditions relative to current hot-wire TWC sensors when the test conditions are at colder temperatures, where BWV is low and therefore has less impact on the IKP2 TWC calculation.

It is recommended that future testing with the IKP2 in SLD conditions be performed at lowest practical temperatures and with multiple MVD sweeps at various fixed LWCs in order to confirm or refute the findings made from this effort in the NASA IRT. Additional research on IKP2 inlet catch efficiency and mass flow calculations are also recommended.

References

1. Strapp, J.W., J. Oldenburg, R. Ide, L. Lilie, S. Bacic, Z, Vukovic, M. Oleskiw, D. Miller, E. Emery, and G. Leone, “Wind tunnel measurements of the response of hot-wire liquid water content instruments to large droplets,” *J. Atmos. and Oceanic Technol.*, Vol. 20, No. 6, 2003, pp. 791-806.
2. Twohy, C.H., Strapp, J.W., Wendisch, M., “Performance of a Counterflow Virtual Impactor in the NASA Icing Research Tunnel,” *J. Atmos. and Oceanic Technol.*, Vol 20, No. 6, 2003, pp. 781-790.
3. Wendisch, M., Garrett, T. J., Strapp, J. W., “Wind Tunnel Tests of the Airborne PVM-100A Response to Large Droplets,” *J. Atmos. and Oceanic Technol.*, Vol. 19, No. 10, 2002, pp. 1577-1584.
4. Miller, D., Potapczuk, M., Bond, T., “Update on SLD Engineering Tools Development,” SAE Technical Paper 2003–01–2127, NASA/TM—2004-213072, April 2004. http://ntrs.nasa.gov

5. Miller, Dean R., Lynch, Christopher J., and Tate, Peter A., "Overview of High Speed Close-Up Imaging in an Icing Environment," NASA/TM—2004-212925, AIAA Paper 2004–0407, 2004.
6. Reehorst, A., Miller, D., Lynch, Bidwell, C., "Total Water Content Measurements With an Isokinetic Sampling Probe," NASA/TM—2010-216217, June 2010.
7. Brenguier J.-L., W. D. Bachalo, P. Y. Chuang, B. M. Esposito, et al., *In Situ Measurements of Cloud and Precipitation Particles. In Airborne Measurements for Environmental Research: Methods and Instruments*, 1st edition by M. Wendish and J.-L. Brenguier. 2013. Wiley-VCH Verlag GmbH & Co. KGaA.
8. Davison, C. R., MacLeod, J. D., Strapp, J. W., and Buttsworth, D. R., 'Isokinetic Total Water Content Probe in a Naturally Aspirating Configuration: Initial Aerodynamic Design and Testing", AIAA Paper 2008-0435, January 2008
9. Strapp, J.W., Lilie, L.E., Ratvasky, T.P., Davison, C., Dumont, C., "Isokinetic TWC Evaporator Probe: Development of the IKP2 and Performance Testing for the HAIC-HIWC Darwin 2014 and Cayenne-2015 Field Campaigns," AIAA Paper 2016-4059, June 2016. doi: 10.2514/6.2016-4059
10. Davison, C., Strapp, J.W., Lilie, L.E., Ratvasky, T.P., Dumont, C., "Isokinetic TWC Evaporator Probe: Calculations and Systematic Uncertainty Analysis," AIAA Paper 2016-4060, June 2016. doi: 10.2514/6.2016-4060
11. Davison, C. R., Benner, M., Landreville, C., and Fuleki, D., "Development and Validation of a Compact Isokinetic Total Water Content Probe for Wind Tunnel Characterization," AIAA Paper 2016-4052, June 2016.
12. Bansmer, S. E., Baumert, A., Sattler, S., Knop, I., Leroy, D., Schwarzenboeck, A., Jurkat-Witschas, T., Voigt, C., Pervier, H., and Esposito, B., "Design, construction and commissioning of the Braunschweig Icing Wind Tunnel," *Atmos. Meas. Tech*., Vol. 11, No. 6, 2018, pp. 3221–3249, https://doi.org/10.5194/amt-11-3221-2018.
13. U.S. Code of Federal Regulations, Title 14, Part 25, Appendix O, Supercooled Large Drop Icing Conditions, 2015 https://rgl.faa.gov/Regulatory_and_Guidance_Library/rgFAR.nsf/0/EDB696E0C079591E86257DC70057179B?OpenDocument
14. Van Zante, J., Riley, J., Strapp, J.W., Esposito, B., et al, "SLD Instrumentation in Icing Wind Tunnels – Investigation Overview," AIAA Paper 2021-2647, August 2021. doi: 10.2514/6.2021-2647
15. King-Steen, L.E., Strapp, J.W., Van Zante, J.F., and Orchard, D., "A Preliminary Study of Inter-Facility LWC Differences in Appendix C and Supercooled Large Droplet Conditions due to Calibration Instruments," AIAA Paper 2021-2652, August 2021. doi: 10.2514/6.2021-2652
16. King-Steen, L., Lilie, L., Bouley, D., "An Examination of Causes of Multi-Wire Bias During SLD Instrumentation Testing in the IRT," AIAA Paper 2021-2653, August 2021. doi: 10.2514/6.2021-2653
17. Lilie, L., Bouley, D., Sivo, C., Ratvasky, T., et al, "Test Results for the SEA Ice Crystal Detector (ICD) under SLD Conditions at the NASA IRT," AIAA Paper 2021-2654, August 2021. doi: 10.2514/6.2021-2654
18. Steen, L.E., Ide, R.F., Van Zante, J.F., "NASA Glenn Icing Research Tunnel: 2014 and 2015 Cloud Calibration Procedures and Results," NASA/TM-2015-218758, May 2015.
19. Rigby, D., Struk, P., Bidwell, C., "Simulation of fluid flow and collection efficiency for an SEA multi-element probe," AIAA Paper 2014-2752, doi: 10.2514/6.2014-2752
20. Bartkus, T.P., Struk, P.M., Tsao, J-C., "Comparisons of Mixed-Phase Icing Cloud Simulations with Experiments Conducted at the NASA Propulsion Systems Laboratory," AIAA Paper 2017-4243, doi: 10.2514/6.2017-4243

21. Strapp, J.W., Schwarzenboeck, A., Bedka, K., Bond, T., et al, "An Assessment of Cloud Total Water Content and Particle Size from Flight Test Campaign Measurements in High Ice Water Content, Mixed Phase/Ice Crystal Icing Conditions: Primary In-Situ Measurements," DOT/FAA/TC-18/1, 2020, http://www.tc.faa.gov/its/worldpac/techrpt/tc18-1.pdf
22. Korolev, A., Isaac, G.A., "Relative Humidity in Liquid, Mixed Phase, and Ice Clouds," *J. Atmos. Sciences*. Korolev Vol 63, No. 11, 2006, pp. 2865-2880. doi.org/10.1175/JAS3784.1
23. Steen, L.E., Ide, R.F., Van Zante, J.F., "An Assessment of the Icing Blade and the SEA Multi-Element Sensor for Liquid Water Content Calibration of the NASA GRC Icing Research Tunnel," AIAA Paper 2016-4051, June 2016. doi: 10.2514/6.2016-4051